

Preparation of $\text{Li}_{4.4}\text{Al}_{0.4}\text{Si}_{0.6}\text{O}_4-x\text{Li}_3\text{BO}_3$ Solid Electrolytes by Sol-Gel Method and Their Ionic Conductivity

LIU, Hua-Ting (刘华亭) CHEN, Ru-Fen* (陈汝芬) SONG, Xiu-Qin (宋秀芹)

Department of Chemistry, Hebei Normal University, Shijiazhuang, Hebei 050016, China

The $\text{Li}_{4.4}\text{Al}_{0.4}\text{Si}_{0.6}\text{O}_4-x\text{Li}_3\text{BO}_3$ ($x = 0$ to 0.5) ion conductors were prepared by the sol-gel method. The powder and sintered samples were characterized by DTA-TG, XRD, SEM and ac impedance techniques. The temperature of the preparation of powder patterns decreased by this method as compared to that of the preparation in solid state reaction. The conductivity and sinterability increased with Li_3BO_3 increasing from $x = 0$ to 0.2 in the $\text{Li}_{4.4}\text{Al}_{0.4}\text{Si}_{0.6}\text{O}_4-x\text{Li}_3\text{BO}_3$ solid electrolytes. The particle size of the sintered pellets is about $0.12 \mu\text{m}$. The maximum conductivity at $20 \text{ }^\circ\text{C}$ is $3.165 \times 10^{-5} \text{ S}\cdot\text{cm}^{-1}$ for $\text{Li}_{4.4}\text{Al}_{0.4}\text{Si}_{0.6}\text{O}_4-0.2\text{Li}_3\text{BO}_3$.

Keywords $\text{Li}_{4.4}\text{Al}_{0.4}\text{Si}_{0.6}\text{O}_4-x\text{Li}_3\text{BO}_3$, ionic conductivity, sol-gel method

Introduction

In the search for new Li^+ ion conducting solids with potential applications as solid electrolytes in high-energy density batteries, considerable work has been done on a variety of Li^+ ion electrolytes. Li_4SiO_4 -based solid solutions are well known for their great increase in conductivity when trivalent Al^{3+} has been substituted by silicon,¹⁻⁶ and maximum conductivity of $\text{Li}_{4+x}\text{Al}_x\text{Si}_{1-x}\text{O}_4$ is obtained at $x = 0.4$.⁷ The conductivity could be considerably increased by the mixing of binders such as Li_3BO_3 glass phase in the solid electrolytes. The reasons for the conductivity improvement have been ascribed to the increased lithium concentration at the grain boundaries and the increased sintering of the pellet.⁸⁻¹⁰

In this research, the $\text{Li}_{4.4}\text{Al}_{0.4}\text{Si}_{0.6}\text{O}_4-x\text{Li}_3\text{BO}_3$ ($x = 0$ to 0.5) ion conductors were prepared by the sol-gel method, and their structure, ionic conductivity and sin-

terability were investigated.

Experimental

General

The compounds were prepared by the sol-gel method using reagent grade Li_2CO_3 , $\text{Al}(\text{NO}_3)_3$, H_3BO_3 , HNO_3 , $\text{Si}(\text{OC}_2\text{H}_5)_4$, and $\text{NH}_3\cdot\text{H}_2\text{O}$. The $\text{C}_2\text{H}_5\text{OH}$ was used as solvent for these materials with $\text{pH} = 5$. The solution was refluxed for 5 h at $86 \text{ }^\circ\text{C}$ and was left at $70 \text{ }^\circ\text{C}$ for gelation. The gels were under vacuum dried and heated gradually from $80 \text{ }^\circ\text{C}$ to $600 \text{ }^\circ\text{C}$ for several hours. The ultra-fine powder was prepared at $600 \text{ }^\circ\text{C}$. The powder was pressed into pellets which were sintered at $650 \text{ }^\circ\text{C}$ for 5 h.

Measurements

The samples were characterized by their powder X-ray diffraction patterns, recorded on a Rigaku/Rotaflex/RINT rotating anode diffractometer using $\text{Cu K}\alpha$ radiation. Thermogravimetric (TG) and differential thermal analysis (DTA) experiments were performed using a Rigaku-TG8101D thermal analyzer at a scan rate of $10 \text{ }^\circ\text{C}/\text{min}$. The shape and size of samples were examined using a scanning electron microscope (SEM). The ionic conductivity measurements were carried out on the sintered samples in the form of pellets, which were polished and painted with Ag PASTE on opposite faces. The ac impedance of the samples was measured using an ac impedance system (EG&G, Princeton Applied Research,

* E-mail: huating@263.net

Received April 11, 2002; revised May 27, 2002; accepted August 5, 2002.

Model 378) that included a potentiostat/galvanostat (Model 273), a lock-in amplifier (Model 5208), and an IBM PS/2 computer. The frequency range was from 5 Hz to 100 kHz. The characterized impedance spectra were simulated with the Equivalent Circuits program developed by A. B. Boukamp.¹¹ The powder was pressed into pellets with a diameter of about 10 mm under a pressure of 120 MPa. Porosity of the pellets was determined by the Archimedes' method.

Results and discussion

Thermal behavior

The DTA-TG curve of Fig. 1 clearly shows the decomposition process of $\text{Li}_{4.4}\text{Al}_{0.4}\text{Si}_{0.6}\text{O}_4 \cdot 0.2\text{Li}_3\text{BO}_3$ gel, which occurs in four steps: the endothermic peak at 80–130 °C is due to the volatilization of H_2O . The endothermic peak at about 170–300 °C is due to the NO_3^- removal by oxidation. The endothermic process at 460–570 °C connects with the reaction of $\equiv\text{Si}-\text{OH} + \text{HO}-\text{Si}\equiv \rightarrow (\text{O}-\text{Si}-\text{O})_n + \text{H}_2\text{O}$.¹² The small peak at 570–600 °C is attributed to the formation of $\text{Li}_{4.4}\text{Al}_{0.4}\text{Si}_{0.6}\text{O}_4$ solid-solution. Relevant TG curve shows the loss of weight. No exothermic and endothermic peaks at high temperatures (> 600 °C) were observed. From the DTA-TG curves, the gel heat-treated temperature were estimated to be 80–600 °C. Other gel samples were similarly in their thermal behavior. The X-ray powder diffraction analysis also indicated that crystals of the products already formed at 600 °C.

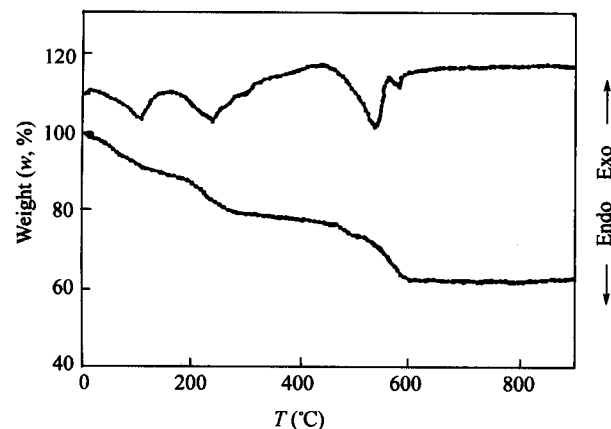


Fig. 1 DTA-TG curve of $\text{Li}_{4.4}\text{Al}_{0.4}\text{Si}_{0.6}\text{O}_4 \cdot 0.2\text{Li}_3\text{BO}_3$ gel.

Structure characterization

Fig. 2 shows the X-ray diffraction (XRD) patterns of $\text{Li}_{4.4}\text{Al}_{0.4}\text{Si}_{0.6}\text{O}_4 \cdot x\text{Li}_3\text{BO}_3$ (a: $x = 0$; b: $x = 0.3$), which have been heated at 600 °C for 6 h. The result of XRD analysis shows that single phase solid solution $\text{Li}_{4.4}\text{Al}_{0.4}\text{Si}_{0.6}\text{O}_4$ in Fig. 2(a) was prepared. The solid solution is isostructural with the monoclinic Li_4SiO_4 . The reflection peaks in the powder diffraction pattern were completely indexed based on a monoclinic symmetry, $P2_1/m$ space group. Meanwhile, the temperature of the preparation of powder patterns is much lower as compared to that of the preparation in solid state reaction (1100 °C).¹³ Li_3BO_3 phase has not appeared for $y = 0.3$ in Fig. 2(b) because Li_3BO_3 has formed glass phase in the $\text{Li}_{4.4}\text{Al}_{0.4}\text{Si}_{0.6}\text{O}_4 \cdot x\text{Li}_3\text{BO}_3$ solid electrolytes. This glass phase could cause synthesis temperature of $\text{Li}_{4.4}\text{Al}_{0.4}\text{Si}_{0.6}\text{O}_4 \cdot x\text{Li}_3\text{BO}_3$ to decrease.

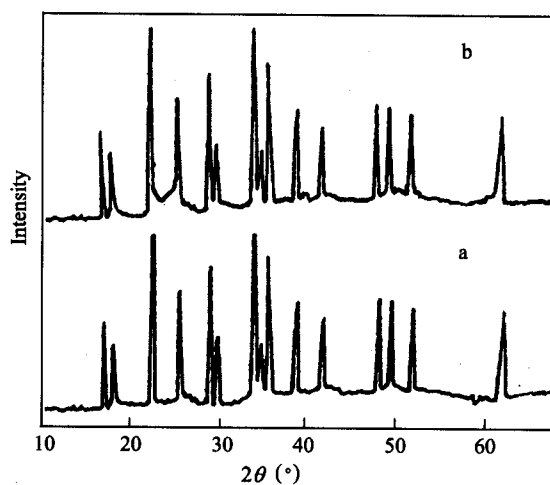


Fig. 2 XRD patterns of $\text{Li}_{4.4}\text{Al}_{0.4}\text{Si}_{0.6}\text{O}_4 \cdot x\text{Li}_3\text{BO}_3$ (a: $x = 0$; b: $x = 0.3$).

Fig. 3 shows the SEM picture of the $\text{Li}_{4.4}\text{Al}_{0.4}\text{Si}_{0.6}\text{O}_4 \cdot 0.2\text{Li}_3\text{BO}_3$ powder by a scanning electron microscope (SEM). From this picture it can be found that the shape of samples is spherical and their average diameter is about 0.12 μm . Other samples have similar shape and size.

Ionic conductivity

The sample powders were pressed into pellets and were heated at 650 °C. The porosity of the sintered pel-

lets for $\text{Li}_{4.4}\text{Al}_{0.4}\text{Si}_{0.6}\text{O}_4-x\text{Li}_3\text{BO}_3$ system is shown in Fig. 4. As can be seen, the porosity tends to have low values with the enhancement of the Li_3BO_3 .



Fig. 3 SEM picture of $\text{Li}_{4.4}\text{Al}_{0.4}\text{Si}_{0.6}\text{O}_4-0.2\text{Li}_3\text{BO}_3$.

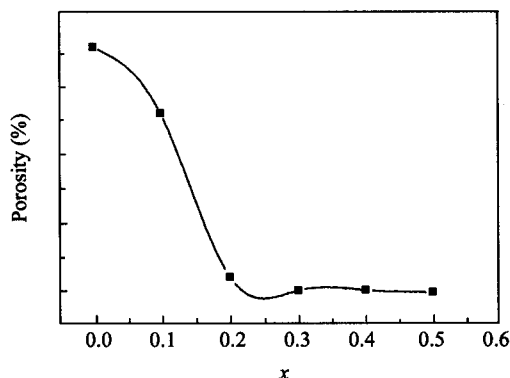


Fig. 4 Variation of the porosity for $\text{Li}_{4.4}\text{Al}_{0.4}\text{Si}_{0.6}\text{O}_4-\text{Li}_3\text{BO}_3$.

The impedance spectra from the electrochemical cell $\text{Ag}/\text{Li}_{4.4}\text{Al}_{0.4}\text{Si}_{0.6}\text{O}_4-x\text{Li}_3\text{BO}_3/\text{Ag}$ were interpreted in terms of three responses that are bulk, grain boundary and Warburg impedance. Typical complex impedance diagram for the $\text{Li}_{4.4}\text{Al}_{0.4}\text{Si}_{0.6}\text{O}_4-0.2\text{Li}_3\text{BO}_3$ measured at 20

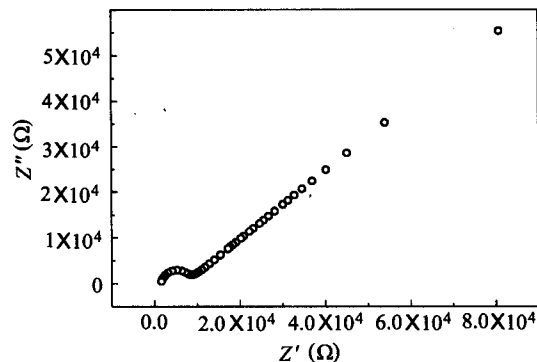


Fig. 5 Complex impedance of $\text{Li}_{4.4}\text{Al}_{0.4}\text{Si}_{0.6}\text{O}_4-0.2\text{Li}_3\text{BO}_3$.

°C is shown in Fig. 5. Similar electric behavior has been observed for all other samples. In Fig. 5, the semicircle in the higher frequency region was attributed to the bulk of grain, while the spike in the low frequency was attributed to the grain boundary.¹⁴ Ionic conductivities of bulk, grain boundary and total for $\text{Li}_{4.4}\text{Al}_{0.4}\text{Si}_{0.6}\text{O}_4-x\text{Li}_3\text{BO}_3$ were obtained from $\sigma = d/R \cdot S$, where d and S express thickness and sectional area of the pellet, respectively.

The ionic conductivities of bulk (σ_1), grain boundary (σ_2) and total (σ) for $\text{Li}_{4.4}\text{Al}_{0.4}\text{Si}_{0.6}\text{O}_4-x\text{Li}_3\text{BO}_3$ systems at 20 °C are shown in Table 1.

It is seen from Table 1 that the ionic conductivity of grain boundary increased with the increase of amount of excess Li_3BO_3 , but conductivity of bulk nearly did not change. The structure of samples has not been changed with increasing of Li_3BO_3 . The addition of Li_3BO_3 glass phase results in the increase of the sintered pellet density, which is very effective for the enhancement of the conductivity of grain boundary. The lithium silicate is formed at the grain boundaries during the heating process, and then the surface of grains are melted and recrystallized by the flux. The second Li_3BO_3 glass phase acts as a flux to accelerate the sintering process and to give high conductivity grain boundaries. Meanwhile, The reason for the

Table 1 Conductivity of bulk, grain boundary and total for $\text{Li}_{4.4}\text{Al}_{0.4}\text{Si}_{0.6}\text{O}_4-x\text{Li}_3\text{BO}_3$

x	0.00	0.10	0.20	0.30	0.40	0.50
$\sigma_1 \text{Li}_{4.4}\text{Al}_{0.4}\text{Si}_{0.6}\text{O}_4-x\text{Li}_3\text{BO}_3 (\times 10^{-5}) (\text{S}\cdot\text{cm}^{-1})$	5.102	6.389	6.353	6.308	6.218	5.206
$\sigma_2 \text{Li}_{4.4}\text{Al}_{0.4}\text{Si}_{0.6}\text{O}_4-x\text{Li}_3\text{BO}_3 (\times 10^{-6}) (\text{S}\cdot\text{cm}^{-1})$	2.862	20.98	63.50	52.97	13.36	10.88
$\sigma \text{Li}_{4.4}\text{Al}_{0.4}\text{Si}_{0.6}\text{O}_4-x\text{Li}_3\text{BO}_3 (\times 10^{-6}) (\text{S}\cdot\text{cm}^{-1})$	1.834	16.69	31.65	28.79	10.997	8.996

conductivity improvement has been ascribed to the increased lithium concentration at the grain boundaries. However, the conductivities of samples decrease at $x \geq 0.3$. Probably the ion moving is obstructed with the amount of Li_3BO_3 increased largely. The maximum conductivity is obtained at around $x = 0.2$ for the $\text{Li}_{4.4}\text{Al}_{0.4}\text{Si}_{0.6}\text{O}_4-x\text{Li}_3\text{BO}_3$ systems examined. Further work will be done in our laboratory.

The temperature dependence of conductivity for $\text{Li}_{4.4}\text{Al}_{0.4}\text{Si}_{0.6}\text{O}_4-0.2\text{Li}_3\text{BO}_3$ is presented in Fig. 6.

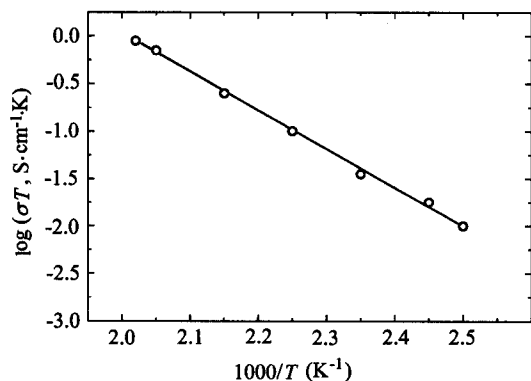


Fig. 6 $\log(\sigma T) - T^{-1}$ relation for the $\text{Li}_{4.4}\text{Al}_{0.4}\text{Si}_{0.6}\text{O}_4-0.2\text{Li}_3\text{BO}_3$.

The values of activity energy were estimated from the equation: $\sigma = A \exp(-E_a/RT)$, where A expresses the pre-exponential factor. The values of activity energy for $\text{Li}_{4.4}\text{Al}_{0.4}\text{Si}_{0.6}\text{O}_4-x\text{Li}_3\text{BO}_3$ systems are shown in Table 2. From Table 2, it can be seen that the higher ionic conductivity of $\text{Li}_{4.4}\text{Al}_{0.4}\text{Si}_{0.6}\text{O}_4-0.2\text{Li}_3\text{BO}_3$ is mainly occasioned by the lower activation energy.

Conclusion

Solid electrolytes, belonging to $\text{Li}_{4.4}\text{Al}_{0.4}\text{Si}_{0.6}\text{O}_4-x\text{Li}_3\text{BO}_3$ ($x = 0$ to 0.5) were prepared by the sol-gel method. The temperature of the preparation of powder patterns is much lower as compared to that of the preparation in solid state reaction. Mixing binders such as Li_3BO_3 glass phase with $\text{Li}_{4.4}\text{Al}_{0.4}\text{Si}_{0.6}\text{O}_4$ are successful in obtaining a high conductivity. The conductivity enhancement by the binder addition resulted mainly from the densification of the sintered pellets. The increase of the lithium content at the grain boundaries is also effective in the conductivity enhancement. The maximum conductivity at $20\text{ }^\circ\text{C}$ is $3.165 \times 10^{-5} \text{ S} \cdot \text{cm}^{-1}$ for $\text{Li}_{4.4}\text{Al}_{0.4}\text{Si}_{0.6}\text{O}_4-0.2\text{Li}_3\text{BO}_3$.

Table 2 The values of activity energy for $\text{Li}_{4.4}\text{Al}_{0.4}\text{Si}_{0.6}\text{O}_4-x\text{Li}_3\text{BO}_3$ systems

x	0	0.1	0.2	0.3	0.4	0.5
E_a $\text{Li}_{4.4}\text{Al}_{0.4}\text{Si}_{0.6}\text{O}_4-x\text{Li}_3\text{BO}_3$ (kJ/mol)	80.0	60.3	42.2	51.4	67.5	71.8

References

- Shannon, R. D.; Taylor, B. E.; English, A. D.; Berzins, T. *Electrochim. Acta* **1977**, *22*, 783.
- Jackowska, K.; West, A. R. *J. Mater. Sci.* **1983**, *18*, 2380.
- Quintana, P.; West, A. R.; West, B. *Ceram. Trans.* **1989**, *88*, 17.
- Quintana, P.; Velasco, F.; West, A. R. *Solid State Ionics* **1989**, *34*, 149.
- Saito, Y.; Ado, K.; Asai, T.; Kageyama, H.; Nakamura, O. *Solid State Ionics* **1991**, *47*, 149.
- Masquelier, C.; Tabuchi, M.; Takeuchi, T. *Solid State Ionic* **1995**, *79*, 98.
- Chen, R. F.; Song, X. Q. *Chin. J. Chem.* **2002**, *20*, 18.
- Tatsumisago, M.; Marita, N.; Minami, T.; Tanaka, M. *Yogyo Kyokai Shi* **1987**, *95*, 197.
- Carette, B.; Ribes, M.; Souquet, J. L. *Solid State Ionics* **1983**, *9/10*, 735.
- Tatsumisago, M.; Yoneda, K.; Machida, N.; Minami, T. *J. Non-Cryst. Solids* **1987**, *95/96*, 857.
- Boukamp, B. A. *Equivalent Circuit. Users Manua & Software* (Ver. 4.51), 2nd edn, University of Twente, The Netherlands, **1993**, p. 18.
- Sun, G.; Yang, S.; Zhang, Z. D. *Huaxue Tongbao* **1990**, *11*, 45 (in Chinese).
- Raistrick, I. D.; Chun, H.; Huggins, R. A. *J. Electrochem. Soc.* **1976**, *123*, 1469.
- Guo, Z. K.; Yan, Y. M. *Chin. Silic. Soc.* **1986**, *14*, 319 (in Chinese).